

## **SCEC PROJECT TECHNICAL REPORT 21100: Constraining a long-term paleolake and paleoseismic history using deep boreholes at the ancient Lake Cahuilla, Coachella, California**

### **Summary**

We collected a 33.5-m-deep continuous borehole near the northeastern end of Lake Cahuilla's shoreline at the Coachella structural depression (CSD) in May 2020 (Fig. 1). This was funded previously by SCEC (20144) and referred to as the CSD core. To estimate the cumulative vertical displacement recorded at CSD and using the funding from this project, we extracted another ~35-m-deep borehole just outside the CSD near Mesquite sand dune (MSD), away from SSAF in June 2021 (Fig. 1). We referred to this core as the MSD core. The detailed stratigraphic log of the borehole suggests approximately 31 lake highstands (water-lain clay/silt rich units), interrupted by sandy units of the fluvial, deltaic, and recessional bar origin (Fig. 2E). Using 13 luminescence and 13 <sup>14</sup>C samples from the sandy and clayey units from the CSD core, respectively, and five new luminescence ages from the MSD core, we are constraining the lake desiccation and highstand cycle of the ancient Lake Cahuilla (Fig. 2E). The corrected luminescence ages show promise (Fig. 3B). However, luminescence ages for the MSD core require additional dating, rigorous fading, and dose rate experiments to account for the apparent stratigraphic age inversion (Fig. 3A). Further, to quantify the variations in the MSD stratigraphy and estimate the water content (e.g., Or and Wraith, 2000; Lukas et al., 2012; Nelson and Rittenour, 2015), we plan to perform an extensive grain-size and shape analysis across the borehole at SDSU's Quaternary Geology Lab. Using the USGS grant (Proposal #: 2022-0032), we also plan to date organic matters from the MSD core for <sup>14</sup>C dating at UC Irvine. Our preliminary age model for the ancient Lake Cahuilla offers the longest lake history (~10.5 ka) to date, including a wealth of structural information associated with the movement on the southern San Andreas Fault (e.g., Philibosian et al., 2011; Rockwell et al., 2018, 2022).

### **Preliminary technical science outcomes**

- Successful extraction of the borehole near Mesquite sand dune at Coachella, Ave. 44, Indio, CA.
- The boreholes record the longest (past ~10.5 ka) lake highstand and desiccation chronology of the ancient Lake Cahuilla.
- At least 31 lake highstands are identified in the MSD core stratigraphic log.
- The five corrected luminescence ages show stratigraphic inversion, suggesting a dire need for additional dating and rigorous dose rate experiments to develop the MSD core's age model.

### **Training, communication, and outreach outcomes**

- The project grant supported the summer salary of one UCLA graduate student.
- One poster and one oral presentation were made during the SCEC 2021 virtual annual meetings and the 2022 SSA Annual Meeting, respectively.
- A manuscript is in preparation for publication in a peer-reviewed journal.

### **Project objective and rationale**

The project's main objective is to test the hypothesis that the lack of surface rupture since the most recent earthquake (MRE) on the southernmost ~100 km of the San Andreas fault (SSAF) is due to Lake Cahuilla's extended dry period. The average earthquake recurrence interval on this stretch of the SSAF in the previous 1000 years is ~180 years. However, the MRE was recorded around 1726±7 A.D., just after the last filling of the ancient Lake Cahuilla in the Salton Trough (Rockwell et al., 2018). Why this stretch of the SSAF remains quiescent for ~300 years is still poorly understood. Some researchers have proposed that lake levels of the ancient Lake Cahuilla modulate the regional stress field (e.g., lake loading and porewater pressure; Luttrell et al., 2007; Brothers et al., 2011) and tie earthquake occurrence to particular lake highstand stages (Rockwell et al., 2018; Rockwell and Klinger, 2019). However, due to limited (~2 ka or younger) lake cycle chronologies as charcoals are sparse and uncertainties in detrital <sup>14</sup>C dates (e.g., reservoir effect on gastropod shells or inheritance of detrital charcoals), the true relationship between loading of the Lake

Cahuilla and earthquake cycles has not been adequately evaluated. Besides, solving this connection is critically important to evaluate fault behaviors such as periodicity, segmentation, characteristic versus random rupture behavior (Weldon et al., 2004), and susceptibility to change in transient pore pressure (Luttrell et al., 2007; Brothers et al., 2011). These parameters are, therefore, critical inputs for earthquake hazard assessment, a key target of SCEC research. They can also significantly improve any future long-term earthquake rupture forecast model's reliability and utility.

### Technical report

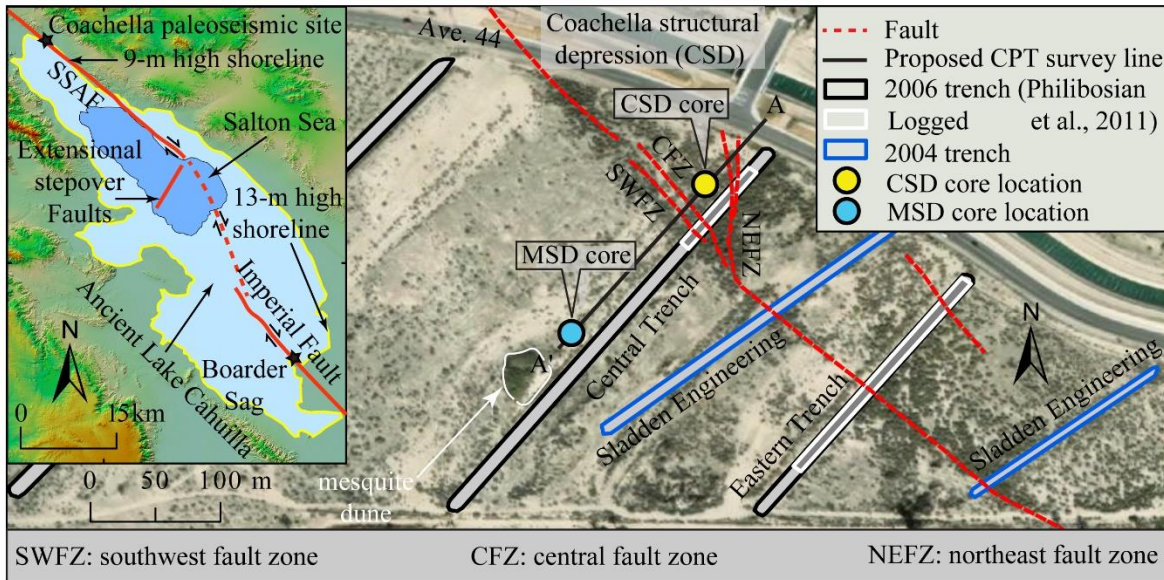


**Figure 1.** Map showing the ancient Lake Cahuilla's 13-m shoreline (inset) and location of the MSD and CSD boreholes relative to the Central Trench of Philibosian et al. (2009, 2011).

Our 2020-21 SCEC research focused on constraining the lake highstand and desiccation cycles of the ancient Lake Cahuilla using a 33-m (CSD core) and ~35-m-deep (MSD core) continuous boreholes. The MSD core is located away from the Coachella structural depression of the Central trench of Philibosian et al. (2011) (Fig. 1). The MSD and CSD cores are well poised to capture more frequent lake fluctuations near the northeastern edge of Lake Cahuilla shoreline and stratigraphic deformation caused by subsidence on the SSAF. The MSD core was extracted using CME-95 continuous core logs and SPT split-spoon sampler (Fig. 2A). To prevent any loss of loose sandy units during extraction, disturbance to the stratigraphy, and limit possible grain mixing, we used 5' x 2.5" transparent plastic liners to recover the MSD core (Fig. 2B).

The individual core segments were immediately warped and capped by double layers of aluminum foils to prevent further sunlight exposure (Fig. 2B). We opened these core segments at UCLA's Luminescence lab under amber lights. We partially dried the core segments and prepared a stratigraphic log of the borehole under amber light before extracting luminescence samples. Later, we split the core segments in half and modified the log under bright light aided by their photomosaics at CSUF (Fig. 2C, D).

Based on the log, we identified at least 31 possible lake highstands based on distinct clayey/silty horizons, following Philibosian et al. (2011) and Waters (1983; Fig. 2). The clayey/silty (lacustrine) horizons are more compact in the bottom core segments than the top, with clearly visible fine laminations, possibly water-lain. The lacustrine units are interrupted by thick sandy horizons. Some sandy and silty units that show finning downward and gradual transition to lacustrine units are interpreted as likely deltaic sedimentation resulting from a rising lake level, followed by clay deposition during the full lake (e.g., Rockwell and Klinger, 2019). Additionally, recessional bars are also sandy and usually well sorted. They are likely more prominent in units that show coarsening downward (Fig. 2). We interpret the gravelly,

coarse, in some cases poorly sorted, sandy matrix as likely fluvial in origin. Fluvial processes in terms of sheet wash deposits are presently dominant at the MSD site. They are also reported from other shoreline environments of Lake Cahuilla (Waters, 1983). Aeolian deposits of fine sands are also expected in some units. We are currently improving our stratigraphic interpretation further using grain size, shape, and thin-section analysis.

We sampled selected sandy units by vertically inserting 6" x 1.5" copper tubes inside the liners, which allowed us to exclude any exposed core materials along the edges. We targeted the sandy units primarily because of the suitable grain size (e.g., 185–220  $\mu\text{m}$ ) required for single-grain p-IR IRSL dating and the longer sunlight exposure assumed for these grains (Rhodes, 2015). Suitable K-feldspar samples (the "Super-K" procedure of Rhodes, 2015) were used to determine equivalent doses ( $D_e$ ). We analyzed approximately 72–152 grains per sample to achieve reasonable certainty and identify the presence of anomalously young grains. Any anomalously young grains are carefully being treated to estimate the accurate  $D_e$  values.

Additional challenges of luminescence dating of borehole samples include asymmetric geologic dose rates due to non-uniform-grain matrix across distinct stratigraphic units (lacustrine vs. subaerial) and varying water content in the geologic past due to fluctuating potentiometric surface at that location (e.g., Brennan, 2006). For example, we targeted the immediate sandy units bounding the lacustrine units to constrain the start of the lake filling and desiccation (Fig. 2). The rationale behind this approach was to reduce any lag time between lake filling and desiccation imposed by erosion and sedimentation rate. However, the dose-rate contribution of finer grains (e.g., clay, silt, fine sand) is different from the coarser grains (e.g., medium and coarse sand) and attenuates with distance. We are working on improving the luminescence age resolution of the MSD core by measuring additional samples for dose rate.

Additionally, water significantly attenuates the track dose from all but the closest grains (e.g., Brennan, 2006). The borehole samples are presently collected from below the groundwater table (i.e., saturated) and are expected to remain saturated in the past. Thus, we estimated the volumetric water content from porosity, assuming that 1) all the pore spaces are completely filled with water and 2) water expulsion likely occurred at depth due to sediment overburden (Or and Wraith, 2000; Lukas et al., 2012; Nelson and Rittenour, 2015). We are currently performing the grain size analysis on the MSD core to estimate the porosity. This will further improve the age resolution of the MSD core. We used the estimated CSD core water content at the corresponding depth to calculate the MSD core luminescence ages.

Another significant source of uncertainty includes anomalous athermal fading of K-feldspar. All our MSD core samples show fading (~2.2–6.3% per decade) at the laboratory timescale (~300 seconds to 3 days). Therefore, we also corrected the fading. However, because the same sample often shows widely variable fading estimates (e.g., J1623: ~2.2–6.0% per decade), additional rigorous fading measurements are crucial to further correct the preliminary ages.

Using the published  $^{14}\text{C}$  ages (Philibosian et al., 2011; Rockwell et al., 2022) and 13 new luminescence ages from the CSD core, and five new single-grain p-IR IRSL ages from the MSD core, we reconstructed the longest lake chronology of the ancient Lake Cahuilla; dating back to ~10.5 ka (Fig. 3).

### **Intellectual merit**

The project offers the longest lake filling and desiccation cycles of the ancient Lake Cahuilla in the Salton Trough. These results are crucial to test whether SSAF is susceptible to lake loading and associated porewater pressure or is just a mere coincidence. In addition, the project has the intellectual merit of offering long-term sedimentologic context for paleoearthquake and slip rate studies in the Coachella Valley. In combination with geotechnical data (e.g., CPT), borehole data also has the potential to estimate the cumulative vertical displacement at the Coachella site. The new luminescence chronology and analytical

improvements are valuable for providing a means to date deep borehole sediments, especially in contexts where no organic material for  $^{14}\text{C}$  exists, or the  $^{14}\text{C}$  ages are enormously affected by inheritance or reservoir effect.

### Broader impacts

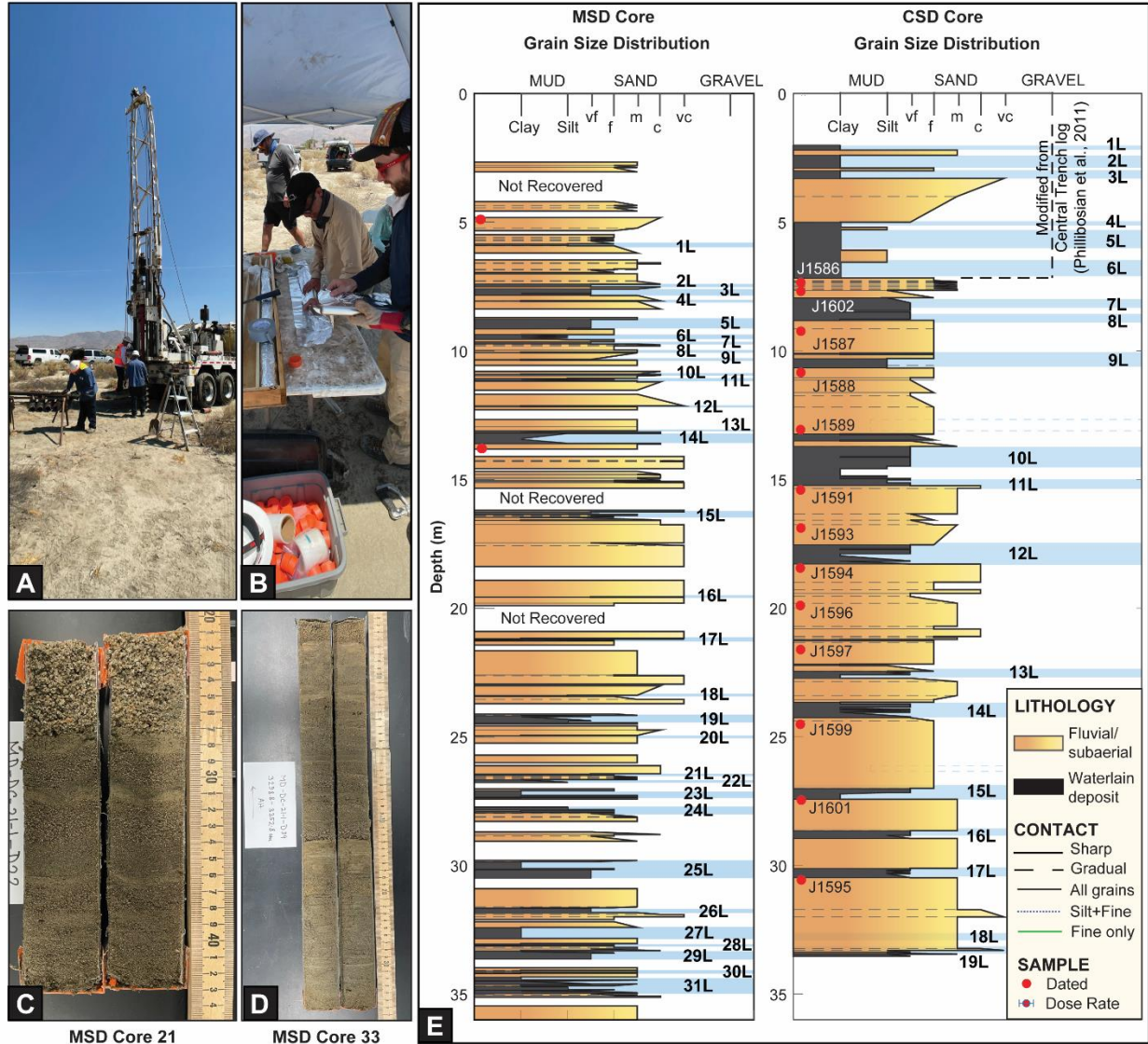


**Figure 2.** Field photos showing the drilling of continuous core segments (A) and wrapping the plastic liners with aluminum foil (B). Photomosaic of core 21 (C) and core 33 (D) highlighting the subtle changes in grain size in the shoreline environment (littoral deposition). (E) Coachella MSD and CSD core stratigraphic logs showing the alternative subaerial sandy and water-lain clayey/silty units. As many as 31 lacustrine units are identified in the ~35-m MSD core. Five luminescence samples were (preliminary) dated from the MSD core to compare with the CSD core and constrain the lake Cahuilla's long-term lake filling and desiccation cycles.

This project has provided ample opportunities for research and training at UCLA, SDSU, & CSUF. The project helps develop a series of other projects for the postdoctoral fellow at the University of Kentucky. A graduate and two undergraduate students are also being trained under this project. This project is part of a Ph.D. thesis at UCLA and two undergraduate research projects at SDSU and CSUF. Besides, the project contributes directly to addressing three primary goals of SCEC5: *Science Objectives* of "P5.b.", "P5.c.", and "P5.d."

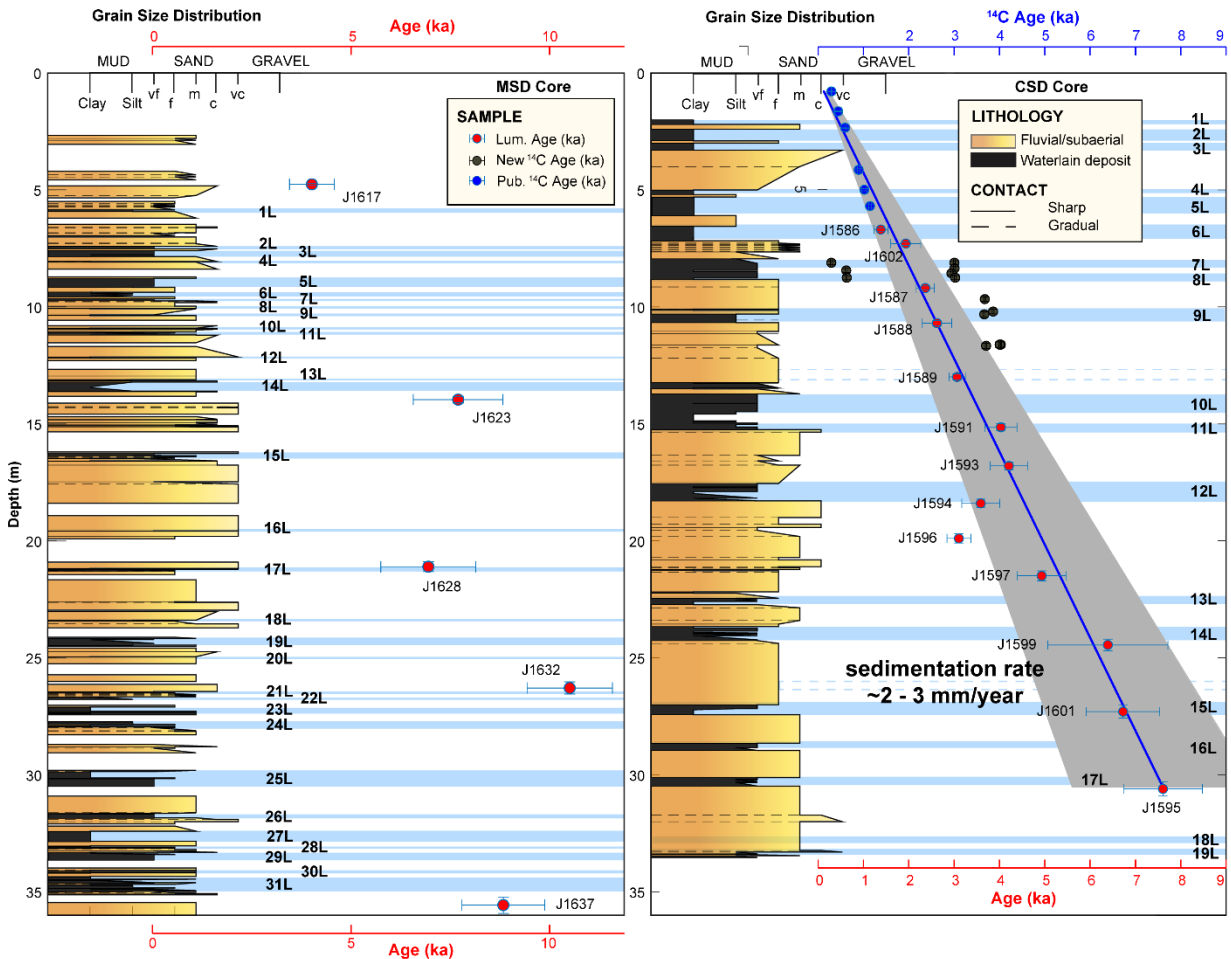


**Figure 3.** Five new single-grain *p*-IR IRSL ages from the MSD core (left) and 13 new luminescence and published (Philibosian et al., 2011; Rockwell et al., 2022), and new <sup>14</sup>C ages from the CSD core (right) are plotted with respect to the borehole's depth. Lake Cahuilla's lacustrine units are highlighted in blue bars. The solid blue line with a gray shaded area shows the average sedimentation rate  $\pm 1\sigma$  (~2–3 mm/year) for the past ~8 ka at the Coachella study site.

## References

- Brothers, D., Kilb, D., Luttrell, K., Driscoll, N., Kent, G. 2011. Loading of the Aan Andreas fault by flood-induced rupture of faults beneath the Salton Sea. *Nat. Geosci.* 4, 486–492. <https://doi.org/10.1038/ngeo1184>.
- Lukas, S., Preusser, F., Flavio, F.S., Tinner, W. 2012. Testing the potential of luminescence dating of high-alpine lake sediments. *Quaternary Geochronology*, 8, 23–32. doi:10.1016/j.quageo.2011.11.007
- Luttrell, K., Sandwell, D., Smith-Konter, B., Bills, B., Bock, Y. 2007. Modulation of the earthquake cycle at the southern San Andreas fault by lake loading. *Journal of Geophysical Research*, 112, 1–15.
- Nelson, M.S., Rittenour, T.M. 2015. Using grain-size characteristics to model soil water content: Application to dose-rate calculation for luminescence dating. *Radiation Measurements*, 81, 142–149. <http://dx.doi.org/10.1016/j.radmeas.2015.02.016>
- Or, D., Wraith, J.M., 2000. Soil water content and water potential relationships. In: Sumner, M.E. (Ed.), *Handbook of Soil Science*. CRC Press, London, pp. 53–85.
- Philibosian, B., Fumal, T.E., Weldon, R.J., Kendrick, K.J., Scharer, K.M., Bemis, S.P., Burgette, R.J., Wisely, B.A. 2009. Photomosaics and logs of trenches on the San Andreas Fault near Coachella, California, in U.S. Geol. Surv. Open-File Report. 2009–1039.
- Philibosian, B., Fumal, T., Weldon, R. 2011. San Andreas Fault Earthquake Chronology and Lake Cahuilla History at Coachella, California. *Bulletin of the Seismological Society of America*, 101, 13–38. <https://doi.org/10.1785/0120100050>.
- Weldon, R. J., Scharer, K. M., Fumal, T. E., Biasi, G. P. 2004. Wrightwood and the earthquake cycle: what a long recurrence record tells us about how faults work, *GSA Today* 14, no. 9, 4–10.

9. Rhodes, E. 2015. Dating sediments using potassium feldspar single-grain IRSL: initial methodological considerations. *Quaternary International* 362, 14–22.
10. Rockwell, T.K., Meltzner, A.J., Haaker, E.C. 2018. Dates of the Two Most Recent Surface Ruptures on the Southernmost San Andreas Fault Recalculated by Precise Dating of Lake Cahuilla Dry Periods. *Bulletin of the Seismological Society of America*, 108, 2634–2649.
11. Rockwell, T.K., Meltzner, A.J., Haaker, E., Madugo, D., White, E. 2019 (in internal review). The Late Holocene History of Lake Cahuilla: Two Thousand Years of Repeated Fillings Within the Salton Trough, Imperial Valley, California. To be submitted to *Quaternary Research*, December 2019.
12. Waters, M. R. 1983. Late Holocene lacustrine chronology and archaeology of ancient Lake Cahuilla, California. *Quaternary Res.* 19, 373–387, doi: 10.1016/0033-5894(83)90042-X.
13. Brennan, B. J. 2006. 2006. Variation of the alpha dose rate to grains in heterogeneous sediments. *Radiation Measurements*, 41, 1026–1031.